Hydrothermal Synthesis, Crystal Structure and Ionic Conductivity of $Ag_2VO_2PO_4$: a New Layered Phosphate of Vanadium(v) †

Hsun-Yueh Kang,[a] Sue-Lein Wang,[a] Ping-Ping Tsai[b] and Kwang-Hwa Lii*[,c]

[a] *Department of Chemistry, National Tsing Hua University, Hsinchu, Taiwan, Republic of China*

[b] *Industrial Technology Research Institute, Materials Research Laboratories, Chutung, Hsinchu, Taiwan, Republic of China*

[c] *Institute of Chemistry, Academia Sinica, Taipei, Taiwan, Republic of China*

A new dioxovanadium(v) phosphate, $Ag_2VO_2PO_4$, has been synthesised hydrothermally at 230 °C and characterized by single-crystal X-ray diffraction. The compound crystallizes in the monoclinic space group $C2/m$ with $a = 12.431(3)$, $b = 6.298(1)$, $c = 6.300(2)$ Å, $\beta = 90.38(2)°$, $Z = 4$ and $R = 0.026$. The structure consists of layers of dimers of edge-sharing VO_6 octahedra and PO_4 tetrahedra, extending parallel to the (001) crystallographic plane with silver ions between the layers. The structural relationship with $BaVO_2PO_4$ is discussed. Alternating current impedance measurements on $Ag_2VO_2PO_4$ indicate that the ionic conductivity at 375 °C is $1 \times 10^{-4}\ \Omega^{-1}\ cm^{-1}$ with an activation energy of 47 kJ mol^{-1}.

Although a large number of new compounds have been synthesised and structurally characterized in the A–V–P–O (A = metal cation) system containing vanadium in oxidation states less than +5,[1-5] considerably less structural work has been reported on the A–V^{5+}–P–O system. To our knowledge, AVO_2HPO_4 ($A = NH_4^+$, K^+, Rb^+ or Tl^+)[6,7] and AVO_2PO_4 ($A = Ba^{2+}$ or Sr^{2+})[8] are essentially the only structurally well characterized examples. The former structure consists of isolated chains of VO_5 square pyramids. Adjacent VO_5 units in each chain are bridged by HPO_4 groups. The latter structure comprises layers of phosphate tetrahedra and edge-sharing bioctahedra, which contain two distorted VO_6 octahedra, with divalent metal cations between the layers.

Attempts to add new members to the A–V^{5+}–P–O system have yielded the layered dioxovanadium(v) phosphate $Ag_2VO_2PO_4$ the structure of which is related to that of AVO_2PO_4 ($A = Ba^{2+}$ or Sr^{2+}). This work reports the hydrothermal synthesis, single-crystal structure, and ionic conductivity of $Ag_2VO_2PO_4$, and forms a part of our programme to search for new solid electrolytes.

Experimental

Synthesis.—A yellow crystalline product was prepared by hydrothermal reaction of Ag_2O (0.309 g), V_2O_5 (0.121 g), H_3PO_4 (0.6 cm^3, 85%) (molar ratio Ag:V:P = 2:1:*ca.* 6), and water (11.4 cm^3) in a Teflon-lined autoclave (23 cm^3) at 230 °C for 4 d followed by slow cooling to room temperature at 5 °C h^{-1}. The product was filtered off, washed with water, rinsed with ethanol, and dried in a desiccator at ambient temperature. Its bulk X-ray powder pattern compared well with that calculated from the single-crystal data. The amounts of Ag, V and P were determined by using an ICP-AE spectrometer after dissolving a sample in dilute nitric acid (Found: Ag, 54.5; P, 7.85; V, 13.1. Calc. for Ag_2O_6PV: Ag, 54.80; P, 7.85; V, 12.95%).

Single-crystal X-Ray Diffraction.—A yellow acicular crystal having dimensions 0.35 × 0.07 × 0.07 mm was selected for indexing and intensity data collection on a Nicolet R3m/V four-circle diffractometer using graphite-monochromated Mo-Kα radiation. Unit-cell parameters and the orientation matrix were determined by a least-squares fit of 17 peak maxima with 2θ ranging from 13 to 30°. Axial oscillation photographs along the three axes were taken to check the symmetry properties and unit-cell parameters. Of the 901 reflections collected ($2\theta_{max}$ = 55°, scan mode 2θ–θ), 550 unique reflections were considered observed [$I > 3.0\sigma(I)$] after Lorentz polarization and empirical absorption corrections. Corrections for absorption were based on ψ scans of a few suitable reflections with χ values close to 90°, using the program XEMP of the SHELXTL-PLUS package.[9] On the basis of intensity statistics and successful solution and refinement of the structure, the space group was determined to be $C2/m$.

The structure was solved by direct methods and successive Fourier synthesis, and refined by full-matrix least-squares refinement based on F values. The multiplicity of the Ag atom was allowed to vary but did not deviate significantly from full occupancy. Therefore, the silver metal site was considered fully occupied in subsequent calculations. The final cycle of least-squares refinement including the atomic coordinates and anisotropic thermal parameters for all atoms converged at $R = 0.0259$ and $R' = 0.0311$. Corrections for anomalous dispersion and secondary extinction were applied. Neutral atom scattering factors for all atoms were used. All calculations were performed on a MicroVax II computer using SHELXTL-PLUS programs. The crystallographic data are listed in Table 1.

Additional material available from the Cambridge Crystallographic Data Centre comprises thermal parameters and remaining bond lengths and angles.

A.C. Impedance Measurements.—Differential thermal analysis was carried out using an Ulvac model 7000 series thermal analyser at temperatures between room and 1000 °C with a heating rate of 20 °C min^{-1}. The sample melted and gave an endothermic peak at 542 °C. A room-temperature powder X-ray diffraction pattern recorded after melting the solid at 550 °C was identical with that before being heated, indicating that $Ag_2VO_2PO_4$ melts congruently at 542 °C. A powder sample (*ca.*, 0.2 g) was pressed at 250 kg cm^{-2} into a disc shape and then sintered at 450 °C in a vacuum-sealed quartz tube. Both

† *Supplementary data available:* see Instructions for Authors, *J. Chem. Soc., Dalton Trans.*, 1993, Issue 1, pp. xxiii–xxviii.

Table 1 Crystal data and intensity collection parameters for $Ag_2VO_2PO_4$

Formula	$Ag_2O_6PV_4$
M	393.7
Crystal system	Monoclinic
Space group	$C2/m$
a/Å	12.431(3)
b/Å	6.298(1)
c/Å	6.300(2)
β/°	90.38(2)
U/Å^3	493.2(2)
Z	4
D_c/g cm^{-3}	5.301
$F(000)$	720
λ(Mo-Kα)/Å	0.710 73
μ(Mo-Kα)/cm^{-1}	98.72
T/°C	24
Scan rate/° min^{-1}	Variable, 2.93 to 14.65 in ω
Scan width/°	1.0 plus Kα separation
2θ range/°	2.5–55
Refined parameters	56
R^a	0.0259
R'^b	0.0311

^{a} $R = \Sigma||F_o| - |F_c||/\Sigma|F_o|$. ^{b} $R' = [\Sigma w(|F_o| - |F_c|)^2/\Sigma wF_o^2]^{\frac{1}{2}}$, $w = 1/[\sigma^2(F) + 0.0010F^2]$.

Table 2 Positional parameters for $Ag_2VO_2PO_4$

Atom	x	y	z
Ag	0.880 65(4)	−0.240 53(6)	0.380 36(6)
V	0.617 07(7)	0	0.087 6(2)
P	0.847 6(1)	0	−0.148 3(2)
O(1)	0.495 8(3)	0	0.206 9(6)
O(2)	0.881 6(2)	−0.196 8(5)	−0.018 9(5)
O(3)	0.723 8(3)	0	−0.177 2(6)
O(4)	0.596 4(3)	½	0.364 5(6)
O(5)	0.701 4(3)	0	0.284 7(6)

Table 3 Selected bond lengths (Å) and bond valence sums (Σs) for $Ag_2VO_2PO_4$

Ag–O(1^{I})	2.436(3)	Ag–O(2)	2.531(3)
Ag–O(3^{II})	2.444(3)	Ag–O(4^{II})	2.226(3)
Ag–O(5)	2.757(4)	Ag–O(5^{III})	2.862(3)
Σs(Ag–O) = 1.05			
V–O(1)	1.689(4)	V–O(1^{IV})	2.318(4)
V–O(2^{V})	1.958(3)	V–O(2^{VI})	1.958(3)
V–O(3)	2.139(4)	V–O(5)	1.620(4)
Σs(V–O) = 4.97			
P–O(2)	1.541(3)	P–O(2^{VII})	1.541(3)
P–O(3)	1.549(4)	P–O(4^{II})	1.534(4)
Σs(P–O) = 4.91			

Symmetry codes: I $\frac{1}{2} + x, -\frac{1}{2} + y, z$; II $\frac{3}{2} - x, -\frac{1}{2} + y, -z$; III $\frac{3}{2} - x, -\frac{1}{2} + y, 1 - z$; IV $1 - x, y, -z$; V $\frac{3}{2} - x, -\frac{1}{2} - y, -z$; VI $\frac{3}{2} - x, \frac{1}{2} + y, -z$; VII $x, -y, z$.

parallel cross-sectional surfaces of the disc were painted with platinum ink as electrode and dried in an oven. The a.c. conductivity measurements were made using a Solartron 1260 Impedance/Gain-Phase Analyzer and a 1286 Electrochemical Interface. Data collection and analysis were carried out with a Hewlett-Packard 9300 desktop computer. Measurements were made mostly in the frequency range 1 Hz to 1 MHz and from room temperature to 410 °C in air.

Results and Discussion

Structure.—The atomic coordinates are listed in Table 2, selected bond distances and bond valence sums[10] in Table 3. The bond valence sums for the cations are in good agreement with their formal oxidation states. The co-ordination number of Ag^+ ion was determined on the basis of the maximum gap in the Ag–O distances ranked in increasing order. The maximum cation–anion distance, L_{max}, according to Donnay and Allmann[11] was also considered. Therefore, the Ag^+ ion has six-co-ordination with the Ag–O bond lengths ranging from 2.226 to 2.862 Å. The shortest Ag–O bond involves the O atom which is not bonded to V. The seventh Ag–O distance is 3.083 Å.

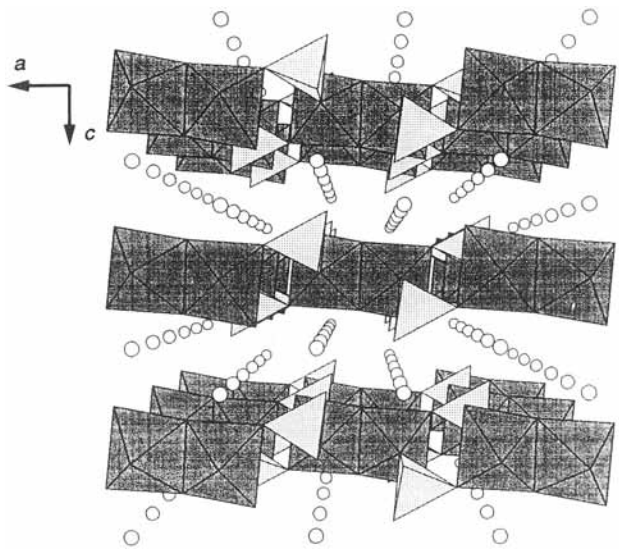

Fig. 1 View of the $Ag_2VO_2PO_4$ structure along the [010] direction showing layers of vanadium phosphorus oxide with Ag^+ ions between the layers

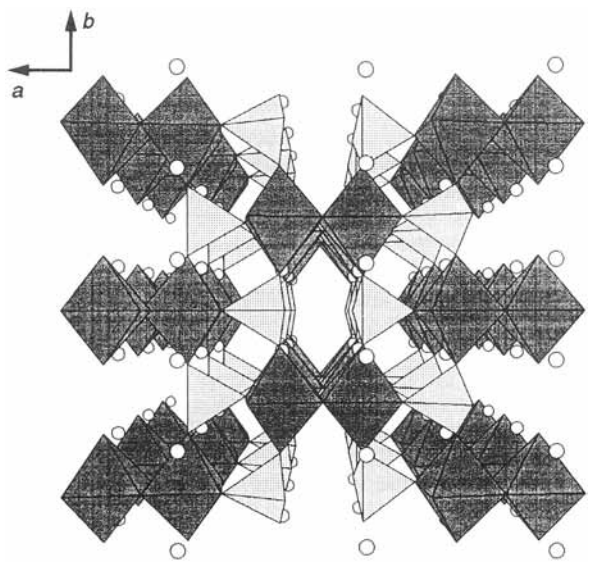

Fig. 2 View of the $Ag_2VO_2PO_4$ structure along [001]

The structure of $Ag_2VO_2PO_4$, viewed approximately parallel to the b axis, is shown in Fig. 1 and contains layers of dioxovanadium phosphate with Ag^+ ions between the layers. Each layer is composed of distorted VO_6 octahedra and PO_4 tetrahedra. There are two types of windows within a layer. One is formed by the edges of two octahedra and two tetrahedra and the other by the edges of four octahedra and two tetrahedra. Straight tunnels with tetragonal and hexagonal windows are formed along the c axis (see Fig. 2). The Ag^+ ions, which occupy sites in the walls of the tunnels, show large thermal parameters indicative of positional disorder.

Two neighbouring VO_6 octahedra form an edge-sharing bioctahedron with a V···V distance of 3.106 Å. Each dimer has a site symmetry of C_{2h} with the mirror plane passing

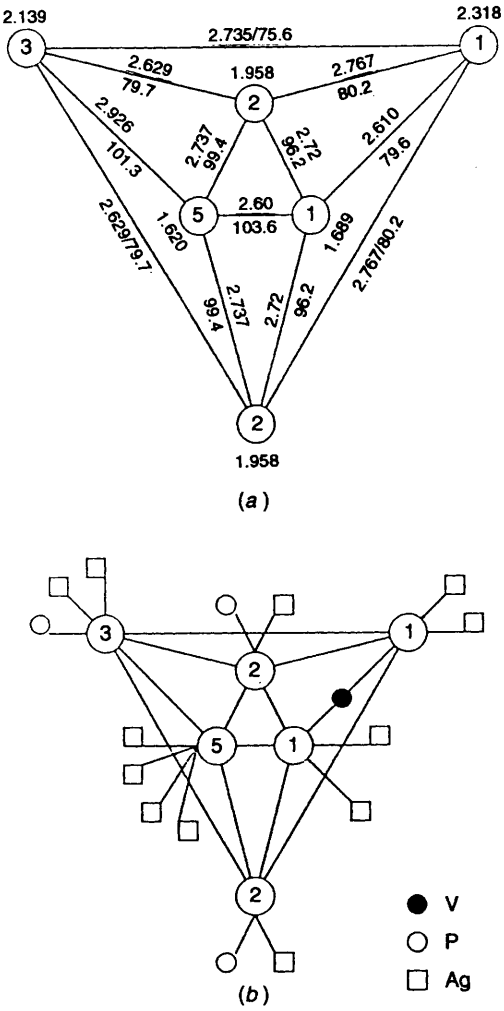

Fig. 3 (*a*) A SCHLEGEL projection of a VO_6 octahedron in $Ag_2VO_2PO_4$. The central V atom is not included. The V–O distances (Å) are given at the terminal positions of the projection. The O • • • O distances and their corresponding angles with respect to the central atom are indicated next to the edges. (*b*) A SCHLEGEL diagram of the co-ordination polyhedron of O around V

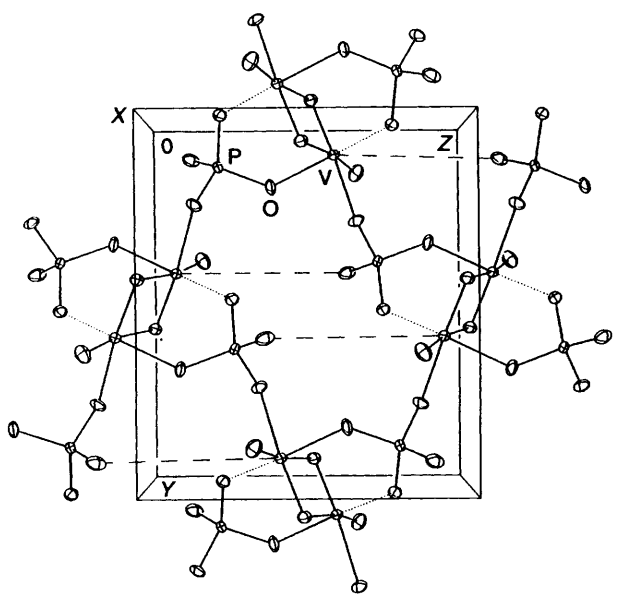

Fig. 4 Transformation of a V–P–O layer in $BaVO_2PO_4$ to that in $Ag_2VO_2PO_4$ by breaking the bonds represented by dotted lines and concomitant formation of those represented by dashed lines

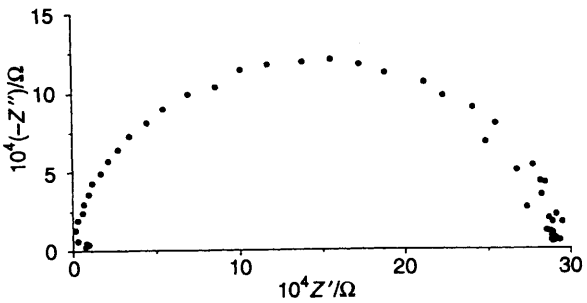

Fig. 5 Semicircle in a complex impedance plane plot for $Ag_2VO_2PO_4$ at 150 °C

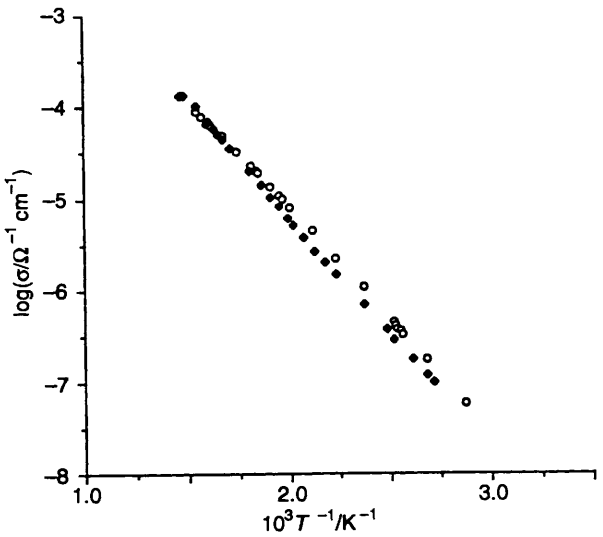

Fig. 6 An Arrhenius plot for $Ag_2VO_2PO_4$ in the temperature range 70–410 °C. Data taken upon heating (●) and cooling (○)

through the V atoms and all the equatorial oxygen atoms. Each VO_6 octahedron consists of two very short, two medium, and two long V–O bond distances. The two very short bonds are *cis* to each other and the bonds *trans* to them are long. Atoms O(2), which are *trans* to each other in axial positions, form two medium-length V–O bonds. Fig. 3 is a SCHLEGEL diagram [12] of the co-ordination polyhedron of O around V in $Ag_2VO_2PO_4$. From the given V–O distances, edge lengths, and the O–V–O bond angles, it is seen that the octahedron is markedly distorted. The edge shared between two octahedra is rather short and the edge *trans* to the common edge is the longest. The two O^{2-} anions forming the common edge of the octahedra are drawn closer together so that the separation of the positive ions is somewhat increased and the two anions better shield the positive charges on the cations. The shortening of the shared edge provides evidence for a predominantly ionic bond. Each phosphate group has three O atoms which are co-ordinated to three neighbouring bioctahedra, and one O atom co-ordinated to Ag^+ ions only. The phosphate tetrahedron is regular as shown by the four nearly equal P–O bond lengths and a narrow range of O • • • O distances (2.48–2.53 Å) within a tetrahedron.

The structure of $Ag_2VO_2PO_4$ is closely related to that of AVO_2PO_4 (A = Ba^{2+} or Sr^{2+}). Both contain layers of phosphate tetrahedra and edge-sharing pairs of VO_6 octahedra. Within a layer in AVO_2PO_4, windows are formed by the edges of four octahedra and four tetrahedra. The divalent cations are located above as well as below each window, the windows being aligned so that straight tunnels are formed. As shown in Fig. 4, a geometrical mechanism which transforms AVO_2PO_4 into $Ag_2VO_2PO_4$ may be envisaged by breaking the bonds represented by the dotted lines with concomitant formation of those represented by dashed lines.

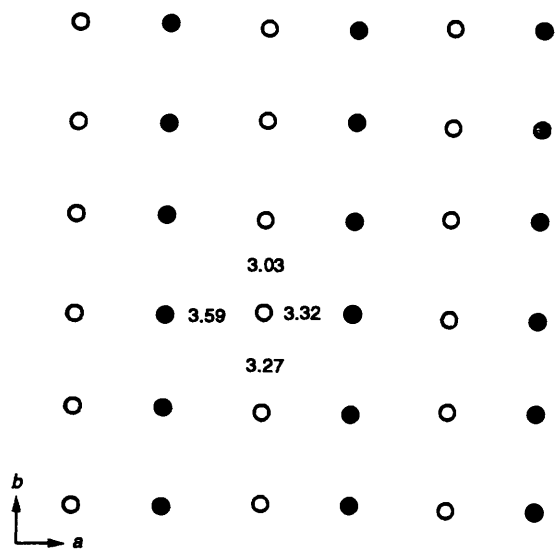

Fig. 7 Projection of a layer of Ag^+ ions in $Ag_2VO_2PO_4$ along [001]. Solid and open circles have different heights along [001]. Distances in Å

Ionic Conductivity.—A representative plot which involves plotting the imaginary part of complex impedance *i.e.* Z'' against the real part, Z', gives one depressed semicircle starting from near the origin (Fig. 5). The results of ionic conductivity measurements of $Ag_2VO_2PO_4$ upon heating and cooling are represented by Arrhenius plots (Fig. 6) according to the equation $\sigma = \sigma_0 \exp(-E_a/RT)$, where σ_0 is the pre-exponential factor, R is the gas constant, and T the absolute temperature. Both heating and cooling data yield straight lines with correlation coefficients greater than 0.999 at temperatures between ≈70 and 410 °C. Below ≈70 °C the conductivity is greater probably due to additional proton conduction. The activation energies obtained from the heating and cooling processes are 48.3 and 46.2 kJ mol^{-1}, respectively. The conduction processes are considered reversible. The activation energy for conduction of Ag^+ is moderate [≈0.5 eV (*ca.* 0.8×10^{-19} J)]. However, the ionic conductivity is only $1 \times 10^{-4}\ \Omega^{-1}\ cm^{-1}$ at 375 °C. As shown in Fig. 7, chains of Ag^+ ions along the *b* axis form puckered layers in the *ab* plane. Consecutive Ag • • • Ag distances within a chain are shorter than those between adjacent chains. The ionic transport is expected to occur within the puckered layers of Ag^+ ions. It would be difficult for Ag^+ ions to conduct through the straight tunnels along the *c* axis because the ions occupy sites in the walls of the tunnels and are at least 6 Å apart. The ionic conductivity of $Ag_2VO_2PO_4$ could be improved by introducing impurities to create more empty sites for Ag^+ ions to occupy. Further research on this material is in progress.

Acknowledgements

Support for this study from the National Science Council, Academia Sinica, and Republic of China Ministry of Economic Affairs (contract no. 38L2320) is gratefully acknowledged.

References

1 H. Y. Kang, W. C. Lee, S. L. Wang and K. H. Lii, *Inorg. Chem.*, 1992, **31**, 4743.
2 K. H. Lii, N. S. Wen, C. C. Su and B. R. Chueh, *Inorg. Chem.*, 1992, **31**, 439.
3 K. H. Lii and L. F. Mao, *J. Solid State Chem.*, 1992, **96**, 436.
4 L. Benhamada, A. Grandin, M. M. Borel, A. Leclaire, M. Leblanc and B. Raveau, *J. Solid State Chem.*, 1992, **96**, 390.
5 L. Benhamada, A. Grandin, M. M. Borel, A. Leclaire and B. Raveau, *J. Solid State Chem.*, 1992, **101**, 154.
6 P. Amoros, D. Beltran-Porter, A. Le Bail, G. Ferey and G. Villeneuve, *Eur. J. Solid State Inorg. Chem.*, 1988, **25**, 599.
7 G. Huan, J. W. Johnson, A. J. Jacobson, E. W. Corcoran, jun. and D. P. Goshorn, *J. Solid State Chem.*, 1991, **93**, 514.
8 H. Y. Kang, S. L. Wang and K. H. Lii, *Acta Crystallogr., Sect. C*, 1992, **48**, 975.
9 G. M. Sheldrick, SHELXTL-PLUS Crystallographic System, Release 4.11, Siemens Analytical X-Ray Instruments, Madison, WI, 1990.
10 I. D. Brown and D. Altermatt, *Acta Crystallogr., Sect. B*, 1985, **41**, 244.
11 G. Donnay and R. Allman, *Am. Mineral.*, 1970, **55**, 1003.
12 R. Hoppe and J. Koehler, *Z. Kristallogr.*, 1988, **183**, 77.

Received 8th December 1992; *Paper* 2/06521E